SPECIALISED IMAGING

RESEARCH ARTICLE

SWIFT and Explosive PIV

UK (Head Office / Factory)
6 Harvington Park,
Pitstone Green Business Park
Pitstone. LU7 9GX England
Tel **+44 (0) 1442 827728**

USA
Specialised Imaging Inc.
40935 County Center Dr. Suite D
Temecula, CA 92591, USA
Tel **+1 951-296-6406**

GERMANY
Hauptstr. 10,
82275 Emmering
Germany
Tel **+49 8141 666 89 50**

specialised-imaging.com **info@specialised-imaging.com**

bsi. ISO 9001:2015 Quality Management
FM 87429

SWIFT and Explosive PIV

Michael J. Murphy*

*W-6 Detonator Technology, Los Alamos National Laboratory, Los Alamos, NM 87545 USA

Abstract. The shock wave image framing technique (SWIFT) and explosive particle image velocimetry (PIV) diagnostics utilize ultra-high-speed imaging to directly visualize explosively-driven motion in condensed, transparent materials. Implementation of a simultaneous SWIFT and explosive PIV diagnostic is currently under development to quantitatively characterize the output of explosive devices by measuring both shock and material mass motion at the same instants in time. The current state of development of the SWIFT diagnostic, as well as the ongoing implementation of explosive PIV, are presented.

Introduction

The shock wave image framing technique (SWIFT) is a mature diagnostic in the Detonator Technology group at Los Alamos National Laboratory for investigating the performance of explosive devices. SWIFT employs spoiled-coherence laser backlighting coupled with schlieren optics to observe the temporal and spatial evolution of shock waves resulting from detonation events confined within transparent media. General system design and implementation has been presented previously[1], and current modes of operation include sub-millimeter-scale for initiator components, millimeter-scale for detonator components, and centimeter-scale for high-expl osive (HE) trains. The ability to directly visualize explosive output using ultra-high-speed frame rates allows the evolution of two-dimensional (2-D) shock-front geometries to be characterized, from which 2-D shock position, displacement, and velocity histories can be obtained.

Explosive particle image velocimetry (PIV) is under development to complement SWIFT by tracking the Lagrangian motion of small tracer particles that propagate with the mass-velocity field moving behind detonation-induced shock waves in transparent materials. Results from initial experiments demonstrate the need for a dynamic, two-dimensional correction to be applied to experimental data in order to correct for optical distortions that arise by viewing the flow-tracing particles through curved shock waves[2]. Implementation of a simultaneous SWIFT and explosive PIV diagnostic is currently underway to utilize the high accuracy and reproducibility of SWIFT data in order to develop appropriate optical corrections for corresponding PIV data. The goal of current research is to develop a diagnostic capable of simultaneously measuring the temporal evolution of shock and corresponding mass motion in two dimensions.

Recent SWIFT data are presented to demonstrate the versatility of the technique over a range of spatial scales, and current designs for the simultaneous SWIFT/explosive PIV diagnostic are discussed, with emphasis on two-dimensional corrections for optical distortion.

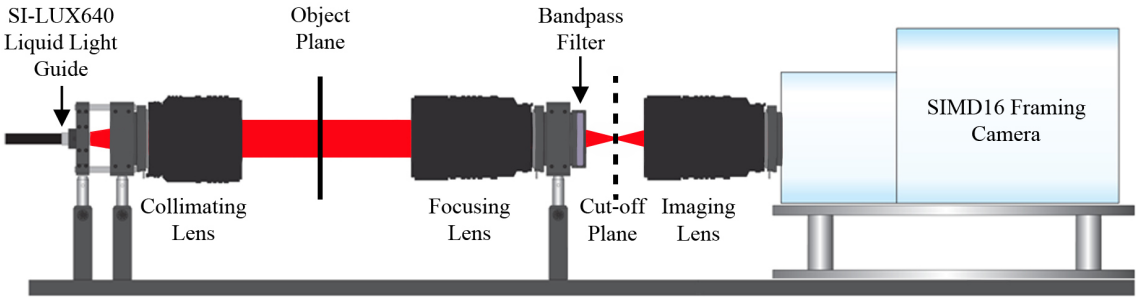

Fig. 1. Representative experimental setup for SWIFT testing.

SWIFT

An optical diagram of a typical SWIFT configuration is displayed in figure 1 for reference. The current SWIFT system employs a SIMD16 ultra-high-speed framing camera paired with an SI-LUX640 high-power diode laser, as described previously[3]. With a numerical aperture of 0.4, a 5 mm-diameter liquid light guide passes 640 $\pm$ 10 nm laser light from the SI-LUX640 laser head to a collimating objective lens. The collimated backlight passes through the object plane to a focusing lens and an imaging lens that work in tandem as an infinity-corrected imaging system. As a result, nominal system magnification (M_0) is determined as the ratio of focal lengths of the imaging and focusing objectives.

Experimental data for intiator, detonator, and HE-scale components are included in figures 2, 3, and 4, respectively, and a list of corresponding lens combinations is provided in table 1 for reference. The image exposure times are kept fixed at 5 ns for all SWIFT experiments.

In figure 2 exploding bridge wire (top) and chip slapper (bottom) initiators are fired into ambient air, and the resulting outputs are visualized in a sub-millimeter field-of-view using 20 ns inter-frame delays. For both cases the camera axis is aligned normal to the direction of electrical current across the metal bridges, and a nominally flat plasma expansion is observed in the direction of the current immediately following bridge burst (second and third image frames). For the chip slapper case, secondary expansion lobes are observed that are thought to result from a combination of plasma expansion due

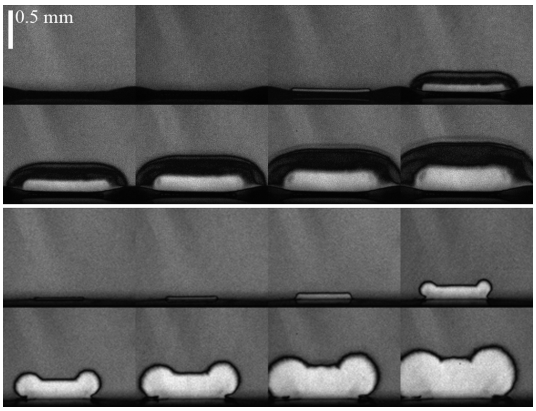

Fig. 2. SWIFT observation of the first 120 ns of (top) exploding bridge wire output and (bottom) chip slapper output into air. A reference image has been subtracted to enhance contrast.

to flyer formation and electrical current focusing. These types of observations in initiator flows are currently unique to SWIFT datasets.

Figure 3 displays detonator output into a polymethylmethacrylate (PMMA) dynamic witness plate using 70 ns inter-frame delays. Centerline shock breakout occurs between the first and second image frames, and the ensuing breakout history over the detonator surface is captured with excellent image quality. Representative methods of analyzing detonator SWIFT data along one-dimensional (1-D) trajectories have been presented previously[4, 1], and are not repeated here. However, it is shown in the ensuing discussion that accurate 2-D shock-front geometries are needed to determine appropriate optical corrections for explosive PIV data. In general, a combination of edge-detection and non-

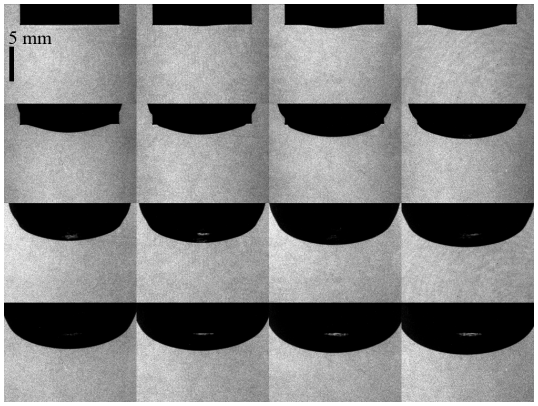

Fig. 3. SWIFT data depicting detonator output into a PMMA dynamic witness plate.

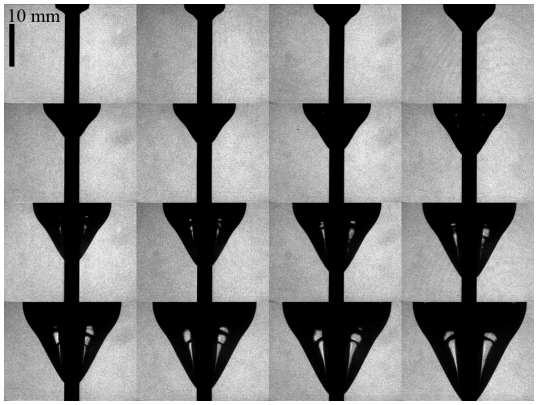

Fig. 4. SWIFT data depicting HE charge output into a PMMA dynamic witness plate.

linear curve-fitting techniques has proven successful in extracting quantitative shock-front geometries from qualitative SWIFT visualizations.

For example, figure 4 depicts the detonation interaction of a 3.5 mm diameter cylindrical charge of extrudable HE confined within PMMA using 190 ns inter-frame delays. As is the case with the detonator data in figure 3, the high-quality images clearly delineate all expanding shock-front positions with excellent image contrast. By combining a Canny edge-detection algorithm with curve-fitting methods similar to historical aquarium-test analysis[5, 6], HE output performance has been successfully characterized for the 3.5 mm diameter HE charge, namely detonation front velocity and radial shock-pressure profiles in PMMA[3].

Collimating Lens	Focusing Lens	Imaging Lens	SWIFT $\sim M_0$
Initiator Scale			
50 mm	105 mm	500 mm	500 / 105
Detonator Scale			
135 mm	300 mm	180 mm	180 / 300
HE Scale			
400 mm	500 mm	60 mm	60 / 500

Table 1. Lens combinations for initiator, detonator, and HE-scale SWIFT configurations.

The efforts underway to implement SWIFT and explosive PIV together to accurately measure the output of explosive devices rely heavily on the observation that SWIFT data is sufficient to not only characterize 2-D explosively-driven shock motion, but the dynamic shock-front geometries as well.

Simultaneous SWIFT/Explosive PIV

A schematic of the current SWIFT/explosive PIV configuration is shown in figure 5, where two ultra-high-speed cameras are required for recording SWIFT and explosive PIV data simultaneously. The camera models under implementation are the SIMD16 manufactured by Specialised Imaging and the Ultra UHSi 12/24 manufactured by Invisible Vision. The UHSi has 7.4 μm square pixels, 1000$\times$880 pixels per image, and 25 lp/mm spatial resolution compared to the SIMD16's 6.45 μm square pixels, 1280$\times$960 pixels per image, and 36 lp/mm spatial resolution. Both cameras record successive images on separate charge-coupled device (CCD) regions with negligible optical errors that affect correlation-based techniques like PIV. In other words, the images can be successfully registered to within sub-pixel accuracy through a combination of in-plane translation, rotation, and scale. Therefore, the SIMD16 is chosen to record PIV data based on its finer pixel size and higher spatial resolution, and the UHSi is employed to record SWIFT images.

A new top-loading explosive boombox has been constructed to provide orthogonal optical viewports that accommodate a PIV laser light sheet propagating orthogonally through the SWIFT backlight, as depicted in figure 5. The PIV illumination source is a custom eight-cavity laser system manufactured by Quantel USA, and general design and performance

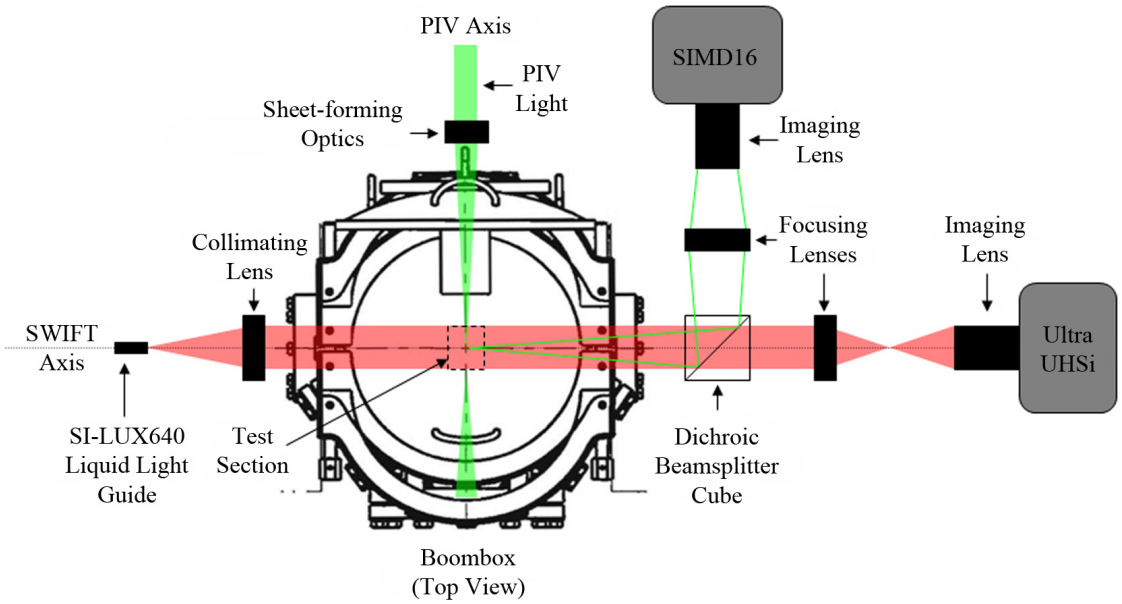

Fig. 5. Experimental setup for SWIFT/Explosive PIV system.

specifications have been described previously[7, 8]. Sheet-forming optics for the PIV laser light sheet are chosen based on a 400 mm standoff distance determined by the size of the boombox, and the resulting light sheet has a nominal height and thickness in the test section of 75 mm and 1 mm, respectively.

For SWIFT and explosive PIV imaging a Nikon 600 mm Nikkor super-telephoto prime lens is employed as the focusing lens, and both imaging lenses are Nikon 300 mm Nikkor super-telephoto units. On the UHSi camera a Tamron $2x$ tele-converter sits between the 300 mm Nikkor lens and the UHSi image plane to counter a 1:0.54 internal system magnification within the camera. A standard dichroic beamsplitter separates and directs the 532 nm PIV light and the 640 nm SWIFT light to each corresponding camera.

The experimental configuration depicted in figure 5 has been fully assembled, and all of the capital equipment is functioning properly. Integration of the UHSi camera into SWIFT is ongoing, and development of experimental timing and triggering procedures are also underway. Development of the SWIFT/explosive PIV diagnostic has been ongoing for multiple years, and the system is expected to be functional within this calendar year.

2-D Optical Correction Development

An in-depth discussion of the development and implementation of a 1-D refraction model based on geometrical optics has been presented previously for correcting PIV data obtained by viewing flow-tracing particles through a curved shock wave propagating within a transparent solid[2]. In this work an extension of the same refraction model is made from 1-D to 2-D configurations in preparation for correcting explosive PIV data. It is important to note that optical distortions due to imaging flow-tracing particles through flat optical ports in the explosive boombox are accounted for through pre-experiment focusing. From the viewpoint of the recording camera the particles are imaged in focus prior to generating a curved shock wave, and that procedure calibrates the imaging system for any static distortion present along the optical path. As a result, the refraction model need only correct for dynamic distortions due to imaging through the shocked volume of the transparent solid. A diagram of the refraction model near the object plane is included in figure 6 for reference.

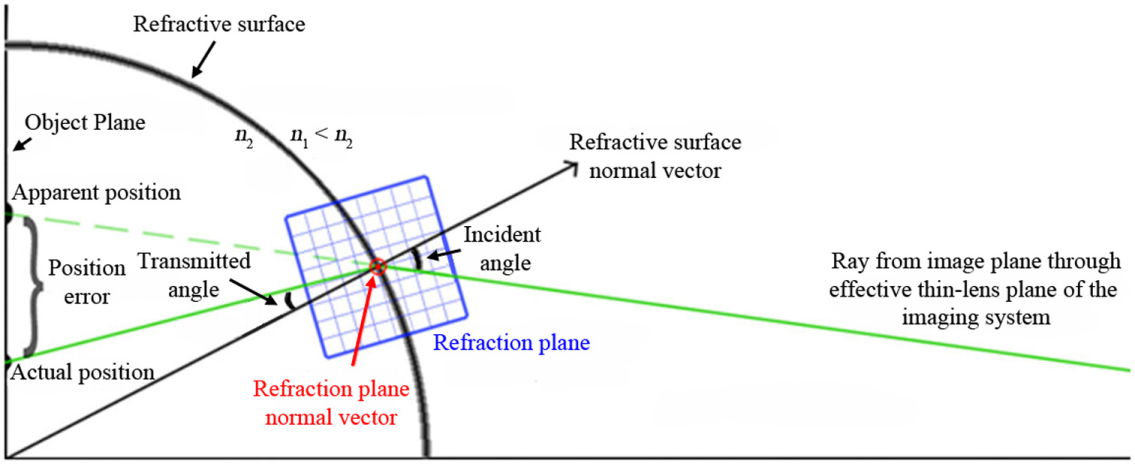

Fig. 6. Diagram of the 2-D refraction model near the object plane.

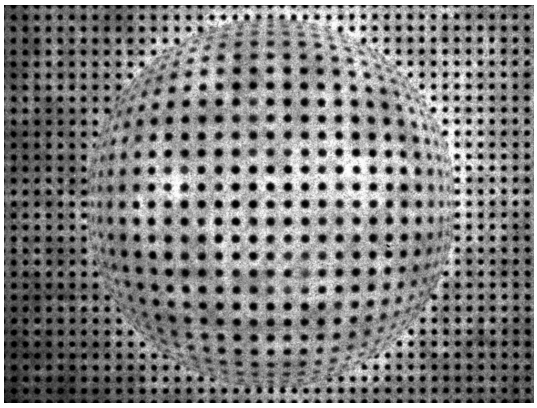

Fig. 7. Image of a dot-grid target viewed through a PMMA hemisphere immersed in ambient air.

The image displayed in figure 7 demonstrates virtual displacements that arise through optical distortion by viewing a fixed-frequency dot-grid target (Edmund Optics #57-983) through a PMMA hemisphere. The target dots have a precise diameter and center-to-center spacing of 0.500 $\pm$ 0.002 mm and 1.000 $\pm$ 0.001 mm, respectively, and the diameter of the PMMA hemisphere is measured as 31.55 $\pm$ 0.005 mm.

Basically, in order to correct for the optical distortion introduced into the imaging system by the PMMA hemisphere, the refraction model equations trace virtual light rays from points in the image plane back to the object plane using knowledge of the imaging setup. Rays that intersect with the hemispherical PMMA surface are refracted according to the jump in refractive index and angle of incidence that occurs at the intersection point, and the calculated refracted rays are traced back to the object plane along straight-line trajectories. In the model, the intersection points of the refracted and non-refracted rays with the object plane denote the actual and apparent positions of the dots, respectively.

With the imaging setup known, i.e. axial locations of the object, image, and objective-lens planes, refraction model calculations are made using the 31.55 mm diameter PMMA hemisphere as the refractive surface. The jump in refractive index across the hemisphere corresponds to light propagating from ambient laboratory air to homogeneous PMMA, and the respective refractive indices are $n_1 = 1.0003$ and $n_2 = 1.49$. As depicted in figure 6, a position error is defined as the distance between the apparent and actual positions in the object plane.

To evaluate the refraction model results, static images of the dot-grid target recorded with and without the PMMA hemisphere are analyzed using a particle-tracking procedure to both identify and locate the target dot positions. Measured position data from the reference and PMMA-refracted images correspond to the actual and apparent dot locations, respectively, and a 2-D field of position errors is calculated and plotted in figure 8. The an-

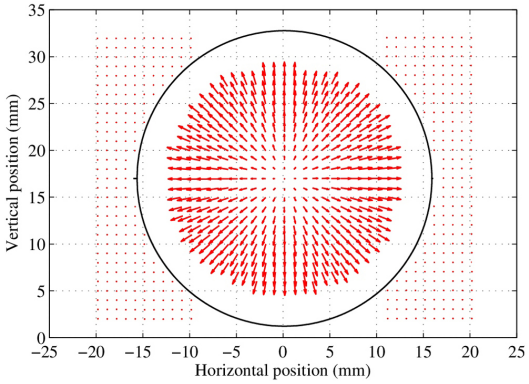

Fig. 8. Measured vector field of position errors due to optical distortion from imaging through a PMMA hemisphere. Solid line contour denotes the circular perimeter of the hemisphere.

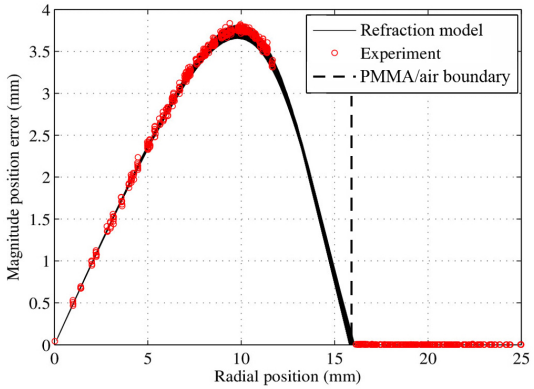

Fig. 9. Position error comparison between experimental and refraction-model results.

nular region of space between the circular perimeter of the PMMA hemisphere and the error vectors corresponds to a region of strong-refraction where dot locations are either not detected or not accurately measured using standard particle-tracking procedures. With such a strong jump in refractive index near the hemispherical perimeter, large angles of light-ray incidence can combine with the refractive-index jump to produce total internal reflection within the PMMA. Consequently, nearly 4 mm of radial position data are not measured from the experimental images.

Since the PMMA refractive surface is hemispherical, the position-error field in figure 8 is reduced to 1-D radial trajectories comparing error magnitude against radial position. A comparison between the results of the refraction model and experimental data is displayed in figure 9, and very good agreement is observed. Quantitatively, by using the calculated position errors from the refraction model to correct the measured (apparent) dot positions, the average difference between the measured reference (actual) positions and the corrected data is less than 30 μm within the PMMA-refracted region. As a result, the 2-D refraction model is currently validated for the case of a static refractive-surface geometry separating homogeneous media, i.e. ambient air and pure PMMA.

Discussion

As the implementation of the simultaneous SWIFT and explosive PIV diagnostic is nearing completion, a set of benchmark tests are being designed to properly characterize the new diagnostic. The main challenge lies in tying SWIFT and explosive PIV data together in order to properly correct for the large, time-dependent, optical distortions that are caused by strong, explosively-driven shock waves having high refractivity in transparent, condensed materials. In other words, significant corrections are expected to be applied to recorded explosive PIV data in order to measure the correct mass velocities, but a benchmark test is required to establish such velocities. Work is progressing along parallel lines to either use standard detonators or small-diameter, cylindrical HE trains to provide validation datasets.

SWIFT images will reliably provide the refractive-surface geometries with high accuracy; however, the resulting surfaces will likely be ellipsoidal rather than spherical, which may challenge the assumption of a constant index of refraction at the perimeter of the refractive surface. Additionally, the static experimental data used to validate the 2-D refraction model have not taken into account the fact that a variable density and refractive index field exist behind real shock waves resulting from detonation interaction. Such shocks are expected to have the highest density at the shock front location with decreasing density as one moves towards the origin. Calculations suggest

that by only modeling refraction at the shock front and assuming homogeneity behind it, the resulting optical corrections should represent a worst-case scenario for calculating the position error for a decaying density field. Quantitative estimates on the severity of the position errors can only be established once benchmark testing has begun.

Efforts are underway to prove out current expectations, and fully integrate SWIFT and explosive PIV for characterizing explosive device performance. Future work is focused on integrating photonic Doppler velocimetry (PDV) into the system as a third orthonormal diagnostic for obtaining direct measurements of mass-velocity history.

Acknowledgments

Funding was provided by the Joint DoD/DOE Munitions Program. The author wishes to thank Joshua Cerimele for assistance with implementation of the 2-D refraction model, Michael Martinez and Dennis Jaramillo for HE firing support, and Steven Clarke for commissioning production of the new explosive boombox. Los Alamos National Lab is operated by Los Alamos National Security, LLC, under Contract No. DE-AC52-06NA25396.

References

1. Murphy, M. J. and Clarke, S. A., "Ultra-high-speed imaging for explosive-driven shocks in transparent media", *D*ynamic Behavior of Materials, Volume 1: Conference Proceedings of the Society for Experimental Mechanics Series, pp. 425–432, 2013.

2. Murphy, M. J., and Adrian, R. J., "PIV through moving shocks with refracting curvature", *Exp Fluids*, Vol. 50, pp. 847–862, 2011.

3. Murphy, M. J. and Johnson, C. E., "Preliminary investigations of HE performance characterization using SWIFT", *Journal of Physics: Conference Series*, Vol. 500, pp. 142024-1–142024-6, 2014.

4. Murphy, M. J. and Clarke, S. A., "Simultaneous phononic Doppler velocimetry and ultra-high speed imaging techniques to characterize the pressure output of detonators", *AIP Conf. Proc.*, Vol. 1426, pp. 402–405, 2012.

5. Johnson, J. N., "Calculated shock pressures in the aquarium test", *A*IP Conf. Proc., Vol. 78, pp. 568–572, 1982.

6. Johnson J. N., Mader C. L. and Goldstein S., "Performance properties of commercial explosives" *P*ropellants, Explosives, Pyrotechnics, Vol. 8, pp. 8–18, 1983.

7. Murphy, M. J., and Adrian, R. J., "PIV space-time resolution of flow behind blast waves", *Exp Fluids*, Vol. 49, pp. 193–202, 2010.

8. Murphy, M. J., Adrian, R. J., and Clarke, S. A., "A particle image velocimeter for measuring the output of high energy detonators", *P*roceedings of the 14th International Detonation Symposium, pp. 482–488, Coeur d'Alene, ID, April 2010.

Question

John Densmore, LLNL
What is the depth of field for the PIV system? How does the depth of field affect the distortion correction and the resulting velocity field?

Reply by Author
Fundamentally any error in the system magnification results in a direct error in the PIV measurement, and the refraction model is effectively correcting for distortion that alters the mapping property (or magnification) of the imaging system. The depth of field is measured to be between 1 and 2 mm, and the laser light sheet thickness is nominally 1 mm. This means the object plane represents particles illuminated in a thin volume that is nominally 1 mm thick in the axial direction of the imaging system. For the static validation case presented in this work the change in system magnification across a 1-2 mm depth of field is negligible compared to the calculated position errors. Optical corrections on the scale of tens of microns may require variable magnification across the depth of field to be addressed, and experimental data is required to evaluate this concern.